

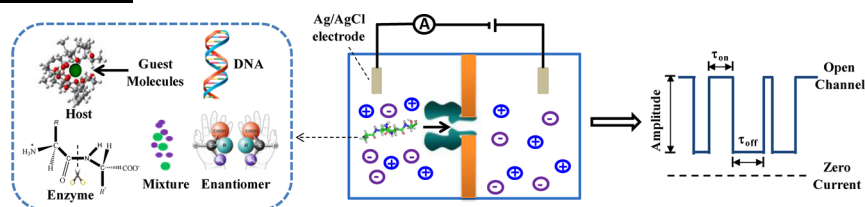
# Nanopore Stochastic Detection: Diversity, Sensitivity, and Beyond

GUIHUA WANG, LIANG WANG, YUJING HAN, SHUO ZHOU,  
AND XIYUN GUAN\*

*Department of Biological and Chemical Sciences, Illinois Institute of Technology,  
Chicago, Illinois 60616, United States*

RECEIVED ON JANUARY 31, 2013

## CONSPECTUS



Nanopore sensors have emerged as a label-free and amplification-free technique for measuring single molecules. First proposed in the mid-1990s, nanopore detection takes advantage of the ionic current modulations produced by the passage of target analytes through a single nanopore at a fixed applied potential. Over the last 15 years, these nanoscale pores have been used to sequence DNA, to study covalent and non-covalent bonding interactions, to investigate biomolecular folding and unfolding, and for other applications.

A major issue in the application of nanopore sensors is the rapid transport of target analyte molecules through the nanopore. Current recording techniques do not always accurately detect these rapid events. Therefore, researchers have looked for methods that slow molecular and ionic transport. Thus far, several strategies can improve the resolution and sensitivity of nanopore sensors including variation of the experimental conditions, use of a host compound, and modification of the analyte molecule and the nanopore sensor.

In this Account, we highlight our recent research efforts that have focused on applications of nanopore sensors including the differentiation of chiral molecules, the study of enzyme kinetics, and the determination of sample purity and composition. Then we summarize our efforts to regulate molecular transport. We show that the introduction of various surface functional groups such as hydrophobic, aromatic, positively charged, and negatively charged residues in the nanopore interior, an increase in the ionic strength of the electrolyte solution, and the use of ionic liquid solutions as the electrolyte instead of inorganic salts may improve the resolution and sensitivity of nanopore stochastic sensors. Our experiments also demonstrate that the introduction of multiple functional groups into a single nanopore and the development of a pattern-recognition nanopore sensor array could further enhance sensor resolution.

Although we have demonstrated the feasibility of nanopore sensors for various applications, challenges remain before nanopore sensing is deployed for routine use in applications such as medical diagnosis, homeland security, pharmaceutical screening, and environmental monitoring.

## Introduction

Understanding of molecular and ionic transport through channels or pores is of paramount interest in many fields such as biology and medical biotechnology. One emerging technique utilized for the experimental study of this important topic is nanopore stochastic sensing. Nanopore sensing can detect analytes at the single-molecule level, in which a nanoscale sized pore (either a biological ion channel

embedded in a planar lipid bilayer or a single artificial pore fabricated in a solid-state membrane) is used as the sensing element.<sup>1</sup> Similar to a Coulter counter,<sup>2</sup> a device for counting microscale particles and cells, nanopore sensors detect analytes based on the ionic current modulations produced by the passage of these substances through the channel bathed in salt solutions at a fixed applied potential (Figure 1). Unlike the electrostatic gating,<sup>3,4</sup> which relies on the electrostatic interaction between the ions and the

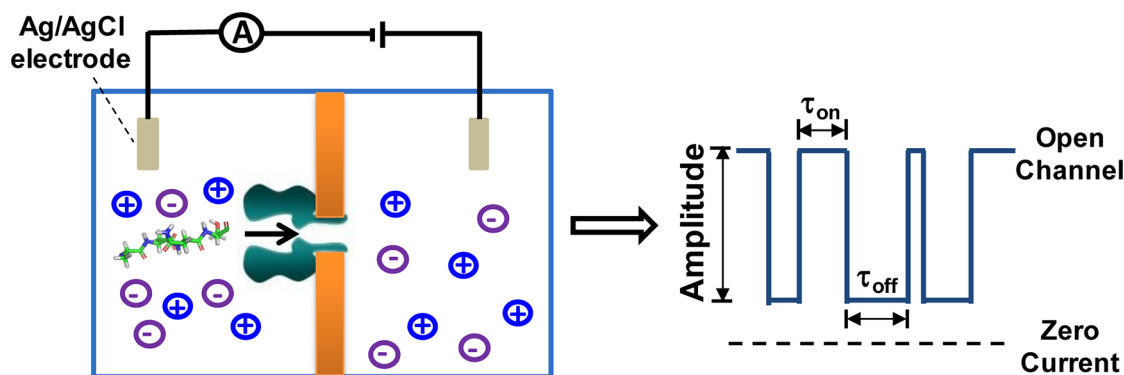


**FIGURE 1.** Schematic representation of the principle for nanopore stochastic sensing.

binding site(s) of the channel to regulate the transport of charged species in the protein ion channels and synthetic pores, nanopore sensors can detect a variety of analytes (charged or uncharged) based on various noncovalent bonding interactions including hydrophobic interactions, aromatic interactions, electrostatic interactions, and hydrogen bonding. The concentration of the analyte can be obtained by the frequency of occurrence ( $1/\tau_{\text{on}}$ ) of the recorded blockage events, while its identity can be determined from the mean residence time ( $\tau_{\text{off}}$ ) of the analyte coupled with the extent of current blockage (amplitude) (Figure 1). Since analytes interact with the binding site of the nanopore one molecule at a time, multiple components in a solution mixture can be quantitated simultaneously using a single nanopore if they produce events having different signatures (i.e., residence times or blockage amplitudes).<sup>5</sup>

The most often used stochastic sensor element is a single transmembrane protein,  $\alpha$ -hemolysin channel. The wild-type  $\alpha$ -hemolysin forms a mushroom-shaped pore, which consists of seven identical subunits arranged around a central axis. The opening of the  $\sim 10$  nm long channel on the *cis* side of the bilayer measures 2.9 nm in diameter and broadens into a cavity of  $\sim 4.1$  nm across. The cavity is connected to the transmembrane domain, a 14-stranded  $\beta$ -barrel with an average diameter of 2.0 nm. Several properties of the  $\alpha$ -hemolysin pore make it unique as a sensor element in stochastic sensing, including known three-dimensional structure, tolerance of structural modification without losing functioning, relatively large single-channel conductance, and quiet open channel without transient background current modulations.

It has been well documented that several factors would strongly affect the translocation of molecules or ions through channels, thus playing important roles in the performance (e.g., resolution and sensitivity) of nanopore

stochastic sensing. These include physical conditions (e.g., pH, voltage, temperature) and the nature (i.e., structural characteristics) of the nanopore.<sup>6–11</sup> Therefore, in order to develop highly sensitive nanopore sensors, two common strategies could usually be employed. The first strategy is structural modification of the nanopore, while the second one involves adjusting the working conditions for the experiment to regulate molecular and ionic transport, thus improving the performance of the nanopore sensor. It should be noted that several substances have been detected based on host–guest interactions.<sup>12–14</sup> However, at present, the majority of the developed nanopore sensors rely on construction of molecular recognition in the nanopore interior, which could be achieved by introducing various surface functional groups such as hydrophobic, aromatic, positively charged, and negatively charged residues inside the nanopore as the binding sites. This sensing principle, which utilizes noncovalent bonding interactions between the well-defined binding site(s) located within the channel interior and the molecules or ions passing through the pore to detect analytes, has been employed for the successful development of ultrasensitive sensors for a wide variety of substances.<sup>10,12,15–21</sup> In addition to their applications in biosensing, these nanoscale sized pores have also offered new possibilities for studying covalent and noncovalent bonding interactions,<sup>22,23</sup> investigating biomolecular folding and unfolding,<sup>24,25</sup> sequencing DNA molecules,<sup>26–32</sup> etc.

Since various aspects of the nanopore stochastic sensing technology have been summarized by many good reviews,<sup>1,33–36</sup> in this Account, we will highlight some of the recent research efforts of our group, especially focusing on the utilization of nanopore sensors for various new applications. Specifically, we will first overview the effort of utilizing nanopore sensing for differentiation of chiral molecules, study of enzyme kinetics, and determination of

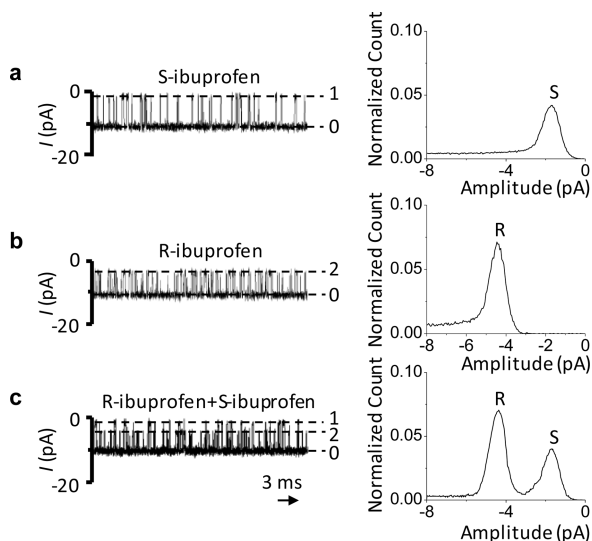


**FIGURE 2.** Current traces showing the interaction of (*R*)- and (*S*)-ibuprofen with the (M113F/K147N)<sub>7</sub>·βCD complex: (A) 20 μM (*S*)-ibuprofen; (B) 20 μM (*R*)-ibuprofen; (C) 20 μM (*S*)-ibuprofen and 20 μM (*R*)-ibuprofen. βCD (40 μM) was added from the *trans* side and ibuprofen from the *cis* side. Recordings were made at −80 mV (*cis* at ground) in 10 mM sodium phosphate buffer, pH 7.4, containing 1 M NaCl. The corresponding amplitude histograms are shown (total counts = 1, unoccupied (M113F/K147N)<sub>7</sub>·βCD state omitted from plot). Reprinted with permission from ref 37. Copyright 2006 American Chemical Society.

sample purity and composition. Then, we will discuss various approaches to regulate molecular transport and improve the sensitivity of nanopore stochastic sensors.

## Applications of Nanopore Stochastic Sensing

**Chiral Molecule Differentiation.** Chiral molecules are nonsuperposable with their mirror images. In many cases, the two mirror images of a chiral molecule (called enantiomers) can act as two different drugs. In general, one enantiomer has a higher degree of potency and a better safety profile than the other, while one enantiomer may cause more side effects than the other. Therefore, the ability to determine which form of a chiral molecule is present in a substance and rapidly quantify the enantiomers of small chiral molecules is critical to the pharmaceutical industry. By using an engineered α-hemolysin protein pore as the sensing element and a host compound β-cyclodextrin as a molecular adapter, Kang et al. have successfully differentiated the *R*- and *S*-enantiomers of two drug molecules, ibuprofen and thalidomide, due to their quite different event blockage amplitudes (Figure 2).<sup>37</sup> It was found that whether β-cyclodextrin and these drug molecules entered the nanopore from the *cis* entrance or via the *trans* opening of the channel affected the enantiomer differentiation significantly. The best separation between the (*R*)- and

(*S*)-thalidomides was achieved when these drug isomers were added to the *trans* side of the pore, while (*R*)- and (*S*)-ibuprofens were best separated when β-cyclodextrin and ibuprofens were added to different sides of the channel. Kang et al. further showed that nanopore stochastic sensing could be a useful tool for kinetic study of racemization. For example, in the absence of human serum albumin (HSA), ~50% of (*S*)-thalidomide was converted into (*R*)-thalidomide or vice versa in ~24 h. In contrast, in the presence of HSA, such a racemization only required ~30–60 min, thus providing evidence that racemization of thalidomides can be catalyzed by HSA.

**Exploring Enzyme Kinetics.** Proteases are involved in a wide variety of physiological processes within living cells. To evaluate their functional roles in complex biochemical networks and for clinical assays, development of a label-free and easy-to-use methodology for the rapid and inexpensive detection of protease–substrate interaction is highly important. Although the feasibility of utilizing nanopores to monitor enzyme activity was demonstrated more than a decade ago,<sup>26</sup> obtaining quantitative chemical kinetics information on enzymatic processes with nanopores is a very recent development in the field of nanopore sensing. One striking example of such an effort was reported by our group, in which an engineered α-hemolysin (M113F)<sub>7</sub> channel was used to study the trypsin cleavage of a fragment of amyloid-β (A-β) peptide (residues 10–20) with a sequence of YEYVHHQKLVFF.<sup>38</sup> We found that in the absence of trypsin, a serine protease to cleave peptide bonds after arginine or lysine amino acid residues, only a single type of blockage event with a large mean residence time and a small residual current was observed, which was due to the substrate, peptide A-β(10–20). In contrast, upon addition of trypsin to the substrate-containing electrolyte solution, two new types of events with shorter residence times and smaller blockage amplitudes were observed, which were attributed to the cleavage products of peptide A-β(10–20) (Figure 3). From the fraction of the events due to the substrate or cleavage products, we could monitor substrate digestion as a function of time. The Michaelis constant,  $K_m$ , and the catalytic rate constant,  $k_{cat}$ , for the reaction between trypsin and A-β(10–20) could further be calculated from the Lineweaver–Burk plot using the frequency of the events produced by the substrate breakdown products. In addition to providing valuable information on enzyme kinetics in real time and without modification of the substrate, another advantage of this nanopore sensing approach is that it could also reveal identities of the cleavage products.

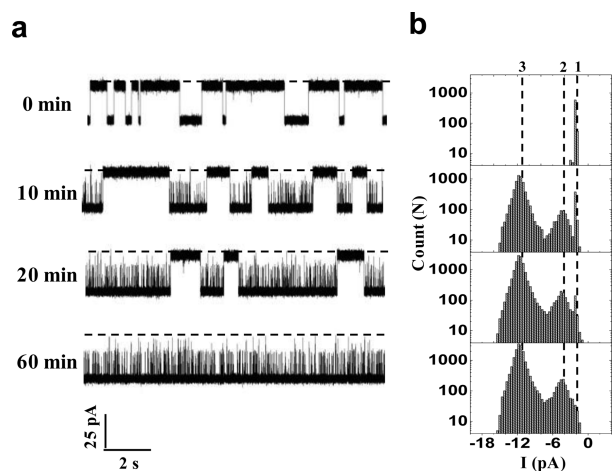


**FIGURE 3.** Monitoring of A- $\beta$ (10–20) cleavage by trypsin. (a) Representative segments of a single-channel recording trace at various times. Dashed lines represent the levels of zero current. (b) Corresponding time-dependent event amplitude histograms. Dashed lines 1, 2, and 3 represent the mean residual current levels for peptides YEVHHQLVFF, YEVHHQK, and LVFF, respectively. Reprinted with permission from ref 38. Copyright 2009 American Chemical Society.

**Detection of Sample Purity and Composition.** The capability for the rapid and sensitive determination of sample purity and composition is highly important in various research areas such as chemical synthesis and pharmaceutical industry. Although numerous detection methods including high-performance liquid chromatography have been developed for this purpose, development of other techniques that can provide more sensitive and less expensive analysis is still desired. The principle for the nanopore determination of sample purity and composition is based on the multianalyte detection capability of stochastic sensing,<sup>5</sup> which permits distinguishable events produced by the interactions between various sample components and the pore. To demonstrate this new application of nanopore stochastic sensing, we studied the interaction between cyclodextrins (CFs) and an engineered  $\alpha$ -hemolysin (M113F)<sub>7</sub> nanopore.<sup>39</sup> CFs are cyclic oligosaccharides, which consist of six or more D-fructofuranose units, and have been used in a variety of applications mainly as consumer product additives and in chromatography. We found that, indeed, CF6 and CF7 produced events with different residence times and blockage amplitudes in the nanopore. Furthermore, both the event residence time and blockage amplitude of CF6 were smaller than those of CF7 (Figure 4), which suggests that CF7 not only has a larger molecular size than CF6 but also could interact more strongly with the (M113F)<sub>7</sub> pore. By establishment of the dose–response curves for CF6 and CF7, the concentrations of these two components could be obtained,

which could then be used to calculate the purity and composition of the sample. To further document this new application of nanopore stochastic sensing, we examined a mixture of cyclodextrin (CD) sample containing  $\alpha$ CD,  $\beta$ CD, and  $\gamma$ CD using the wild-type  $\alpha$ -hemolysin pore. Again, we observed three types of events with significantly different mean residence times and residual currents. Therefore, accurate determination of the purity and composition of the CD sample could be accomplished.

## Improving the Sensitivity of Nanopore Sensors

**Construction of Noncovalent Bonding Sites in the Nanopore Interior.** As discussed in the Introduction, it has been well established that the resolution and sensitivity of stochastic sensing is largely dependent on the nature of the nanopore. Therefore, structural modification of the nanopore to introduce a variety of new functional groups in the nanopore interior to regulate the transport of target analytes provides an effective means to increase the nanopore sensitivity and selectivity. To demonstrate this concept, we investigated peptide translocation in three  $\alpha$ -hemolysin pores including the wild-type (WT)<sub>7</sub> as well as mutants (M113F)<sub>7</sub> and (2FN)<sub>7</sub>.<sup>5</sup> Note that the (M113F)<sub>7</sub> pore has an aromatic binding site (containing seven aromatic phenylalanine side chains at position 113) for aromatic molecules, while in addition to these seven phenylalanine residues, the (2FN)<sub>7</sub> pore has seven additional phenylalanine amino acids at position 145.

Figure 5 shows the electrical recording traces as well as residual current and mean residence time plots for peptide Y6 (consisting of six aromatic tyrosine amino acids) in the three  $\alpha$ -hemolysin protein pores. It is apparent that the translocation of Y6 in the (WT)<sub>7</sub>  $\alpha$ -hemolysin protein produced much shorter duration events and had a much smaller formation constant than its transport in the other two mutant pores. The significant difference in the event residence time and formation constants observed in the three  $\alpha$ -hemolysin pores may be attributed to the weak hydrophobic interactions occurring between the peptide and the (WT)<sub>7</sub> pore, while additional aromatic interactions were involved with peptide Y6 and the other two mutant, (M113F)<sub>7</sub> and (2FN)<sub>7</sub>, pores. Further, we noticed that, with more aromatic residues engineered inside the lumen of the protein pore (i.e., (2FN)<sub>7</sub> pore vs (M113F)<sub>7</sub> pore), a stronger binding affinity between the peptide and the pore was observed. Taken together, the combined results suggest that the functional groups engineered inside a protein pore are responsible for

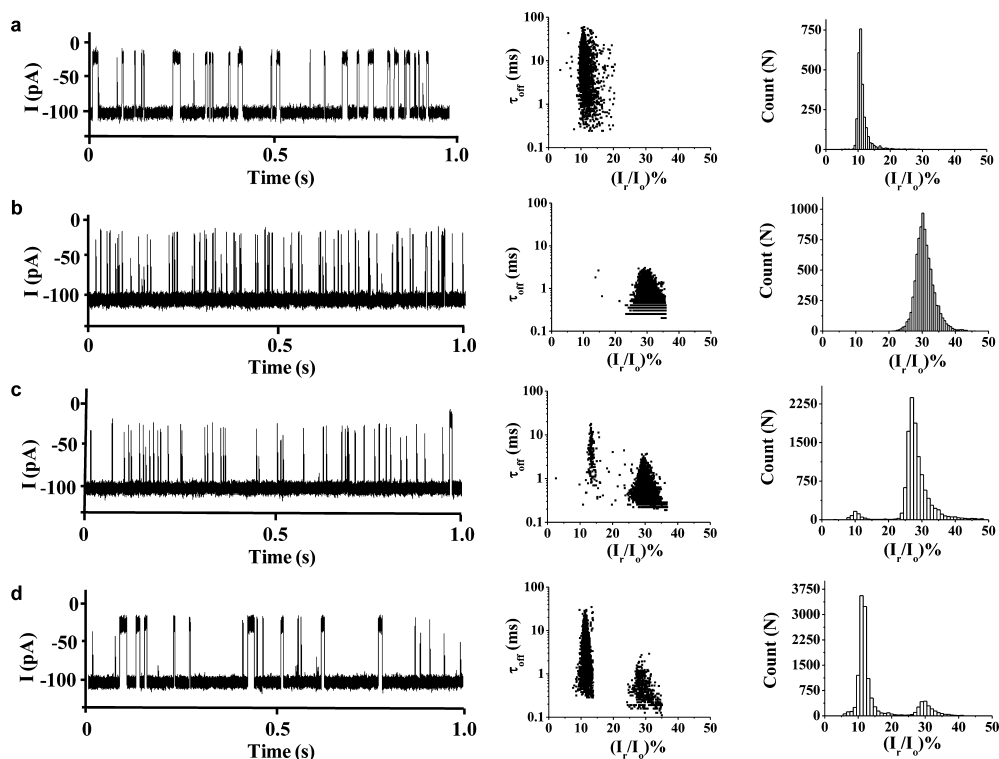


**FIGURE 4.** Nanopore detection of cyclofructans: (a) CF7 (>99% pure); (b) CF6 (>99% pure); (c) CF6 (95%) + CF7 (5%); (d) CF6 (15%) + CF7 (85%). (left) Typical single channel current recording traces; (middle) the corresponding scatter plots of event amplitude vs residence time; (right) the corresponding event amplitude histograms.  $I_r/I_o$  in the middle and right panels is normalized blockage residual current, which was obtained by dividing the average blockage residual current of an event by the average open channel current. Reprinted with permission from ref 39. Copyright 2011 Royal Society of Chemistry.

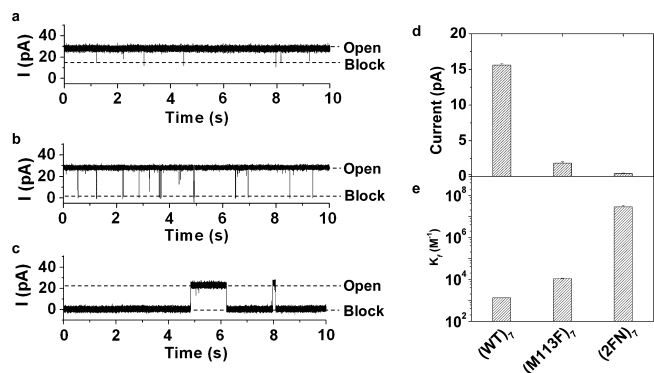


**FIGURE 5.** Effect of the structure of protein pores on peptide translocation. Typical single-channel recording traces: (a) (WT)<sub>7</sub>, (b) (M113F)<sub>7</sub>, and (c) (2FN)<sub>7</sub>, showing the interaction between peptide Y6 and three different protein pores; (d) event residual currents; (e) formation constants  $K_f$ . Reprinted with permission from ref 5. Copyright 2009 American Chemical Society.

the affinities between peptides and the protein ion channel, thus predominantly determining the sensitivity and the resolution of the stochastic nanopore sensor. With the much enhanced resolution of the engineered protein pore, we successfully differentiated a series of short peptides, including those differing by only one amino acid. The feasibility of

utilizing the engineered protein pore for simultaneous detection of a mixture of peptides (Figure 6) and even differentiation of peptide sequences was further demonstrated.

It should be mentioned that, in the various nanopore stochastic sensors developed so far, the sensing element usually possesses a binding site that contains a single or several identical functional groups. Nanopore sensors made by such a modification strategy sometimes could not provide an enough resolution for analyte differentiation. For example, Wang et al. reported a rapid sensor to detect cyclohexyl methylphosphonic acid (CMPA) and pinacolyl methylphosphonate (PMPA), hydrolytes of nerve agents soman and cyclosarin, respectively, by using the (M113F/K147N)<sub>7</sub> protein pore and  $\beta$ -cyclodextrin as a molecular adapter.<sup>40</sup> Although this sensor is very sensitive, with detection limits of the order 100 nM or better, CMPA and PMPA could not be differentiated due to their similar event residence times and blockage amplitudes. Recently, Gupta et al. designed a multifunctionalized  $\alpha$ -hemolysin pore, (M113K)<sub>3</sub>(M113Y-D8)<sub>4</sub>, for the successful differentiation and simultaneous quantification of CMPA and PMPA, in which two different functional groups (lysine and tyrosine)

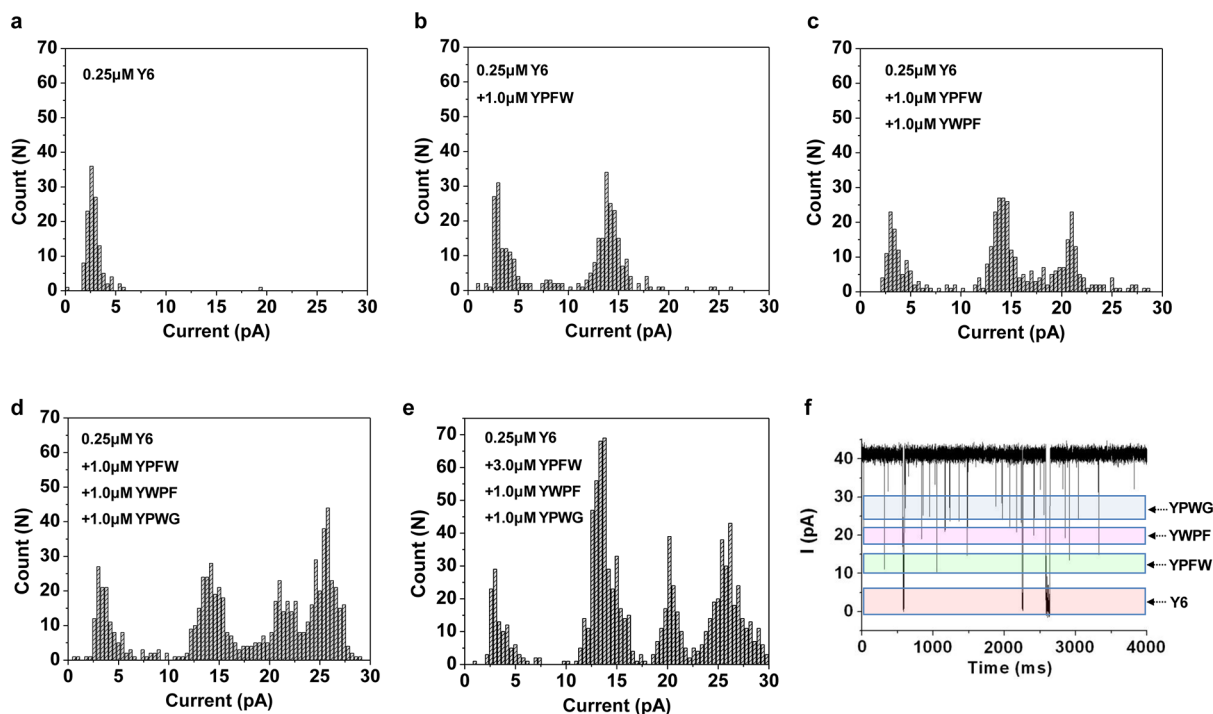


**FIGURE 6.** Simultaneous detection of a mixture of peptides. Event histograms of (a) peptide Y6; (b) a two-peptide mixture containing Y6 and YPFW; (c) a mixture of three peptides containing Y6, YPFW, and YWPF; (d) a mixture of four peptides containing Y6, YPFW, YWPF, and YPWG; (e) a mixture of Y6, YPFW, YWPF, and YPWG where the concentration of YPFW was three times larger than that of the mixture in panel d; and (f) the corresponding representative single-channel current trace of panel d, in which the individual Y6, YPFW, YWPF, and YPWG events were arrow-marked at different levels. Reprinted with permission from ref 5. Copyright 2009 American Chemical Society.

were concurrently introduced within the interior of a single  $\alpha$ -hemolysin pore.<sup>41</sup> In this (M113K)<sub>3</sub>(M113Y-D8)<sub>4</sub> pore, the function of the four M113Y-D8 subunits is to hold the  $\beta$ -cyclodextrin host tightly inside the channel, which could then capture CMPA/PMPA, while the three positively charged lysine residues in the M113K subunits may interact with the polar phosphonate group of CMPA/PMPA, thus improving the organophosphate differentiation resolution. This multifunctionalized nanopore approach provides new strategies for future nanopore sensor design.

**Increasing the Concentration of Electrolyte Solutions.** It is well-known that ionic strength affects the rates of chemical reactions, particularly those involving charged particles. To investigate the feasibility of utilizing the salt effect to improve the resolution and sensitivity of the nanopore sensor, we studied the effect of ionic strength on three types of noncovalent bonding interactions (electrostatic, aromatic, and hydrophobic interactions) by monitoring the interactions between three types of analytes and three  $\alpha$ -hemolysin protein pores having different binding sites.<sup>23</sup> Our experimental results showed that with an increase in the ionic strength of the electrolyte solution, the association rate constants of both hydrophobic and aromatic interactions

were retarded, while that of the electrostatic interaction was accelerated (Figure 7). This suggests that the salt effect on the rate of association of analytes to a pore differs significantly depending on the nature of the noncovalent interactions occurring in the protein channel. On the other hand, as the ionic strength increased, dramatic decreases in the dissociation rate constants were observed for all three types of noncovalent bonding interactions studied, resulting in significant increases in the overall reaction formation constants. This result suggests that the salt effect indeed can be used as an effective approach to significantly increase the resolution and sensitivity of the nanopore stochastic sensor. Hence, variation of the salt concentration may find useful application in stochastic sensing, for example, in the analysis of small molecules, and in the differentiation and even simultaneous detection of a mixture of structurally similar compounds.

**Use of Ionic Liquid Solutions as the Electrolytes.** Nanopore experiments are usually performed in large concentrations of inorganic salt solutions such as 1 M NaCl or 1 M KCl. As discussed in the Introduction, in addition to the nature of the nanopore, physical conditions also play important roles in transporting molecules and ions through channels. For example, various experimental parameters such as voltage,

temperature, and pH of the solution have been used as an effective means to regulate molecular transport.<sup>6–8</sup> Recently, our group investigated the feasibility of utilizing other salt solutions such as ionic liquids (generally containing bulky organic cations) instead of the commonly used NaCl/KCl as the background electrolytes in nanopore

sensing to improve nanopore resolution. In our experiments, the interaction between boromycin and the  $\alpha$ -hemolysin protein pore was monitored in 1 M NaCl and 1 M ionic liquid butylmethylimidazolium chloride (BMIM-Cl) solutions. We found that the events in 1 M BMIM-Cl solution showed a 2.6-fold larger mean residence time than those in 1 M NaCl solution ( $8.54 \pm 0.04$  ms versus  $3.29 \pm 0.04$  ms).<sup>13</sup> A similar observation has been made by Modi et al. in their study of the interaction of ampicillin with the outer membrane porin F (OmpF), where a 1 M BMIM-Cl solution increased the residence time of ampicillin by a factor of 3 compared with a KCl solution of the same concentration.<sup>42</sup>

The feasibility of utilizing aqueous solutions of ionic liquids to slow single-stranded DNA (ssDNA) translocation through the nanopore was then further investigated. It should be noted that one of the most prominent potential applications of nanopore technology is DNA sequencing. In nanopore DNA sequencing, ssDNA molecules are electrophoretically driven through a nanochannel; the discrimination of polynucleotides might be achieved based on their different current signatures in the pore (e.g., residence times or current blockage amplitudes). Unfortunately, one of the major hurdles of utilizing nanopores to sequence ssDNA molecules is their rapid translocation velocity ( $\sim 1\text{--}3$   $\mu\text{s}/\text{base}$ ) through the nanopore,<sup>27</sup> which prevents the detection of the local structure or sequence of the freely translocating DNA via ionic current measurement. To slow and control DNA translocation, a number of techniques have been

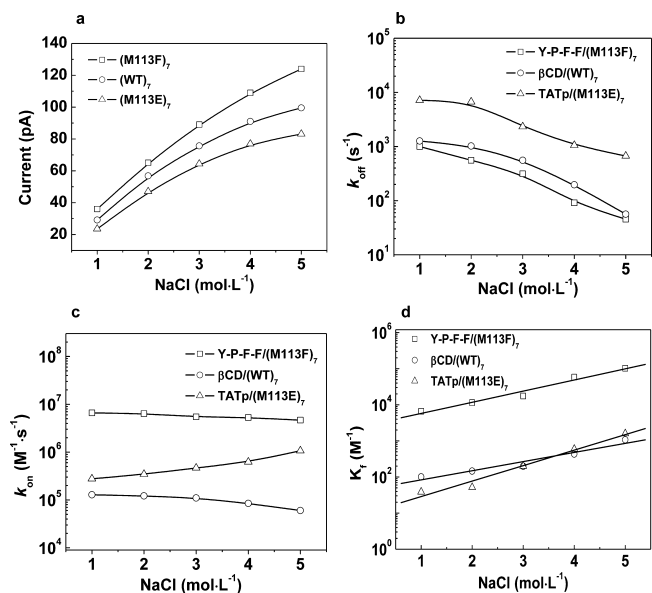


**FIGURE 7.** Dependence of the open channel currents of protein pores and the kinetic constants of the noncovalent interactions on the salt concentration. (a) Open channel currents; (b) association rate constants,  $k_{\text{on}}$ ; (c) dissociation rate constants,  $k_{\text{off}}$ ; and (d) reaction formation constants  $K_f$ . Reprinted with permission from ref 23. Copyright 2008 The Biophysical Society.

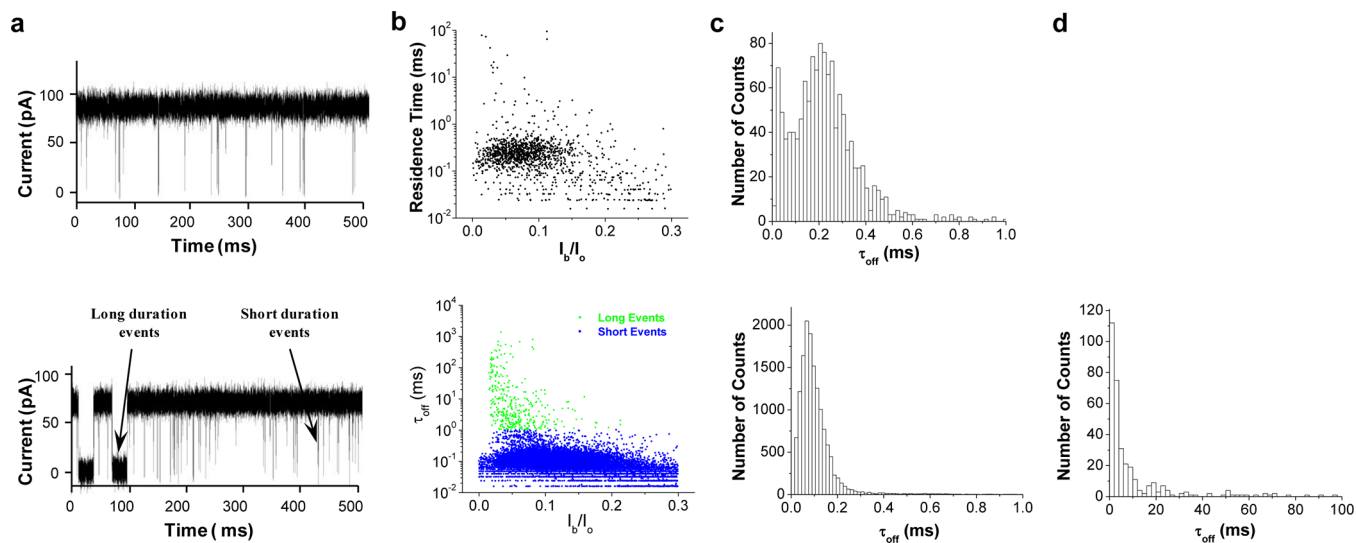


**FIGURE 8.** Translocation of  $(\text{dA})_{20}$  in the mutant  $(\text{M113F})_7\alpha\text{HL}$  pore in 1 M NaCl (upper panel) and 1 M BMIM-Cl (lower panel). (a) Representative single channel current recording trace; (b) scatter plot of event amplitude vs residence time; (c) residence time histogram of short-lived events; and (d) residence time histogram of long duration events.  $I_b/I_o$  in panel b is normalized blockage residual current, which was obtained by dividing the average blockage residual current of an event by the average open channel current. Reprinted with permission from ref 43. Copyright 2009 American Chemical Society.

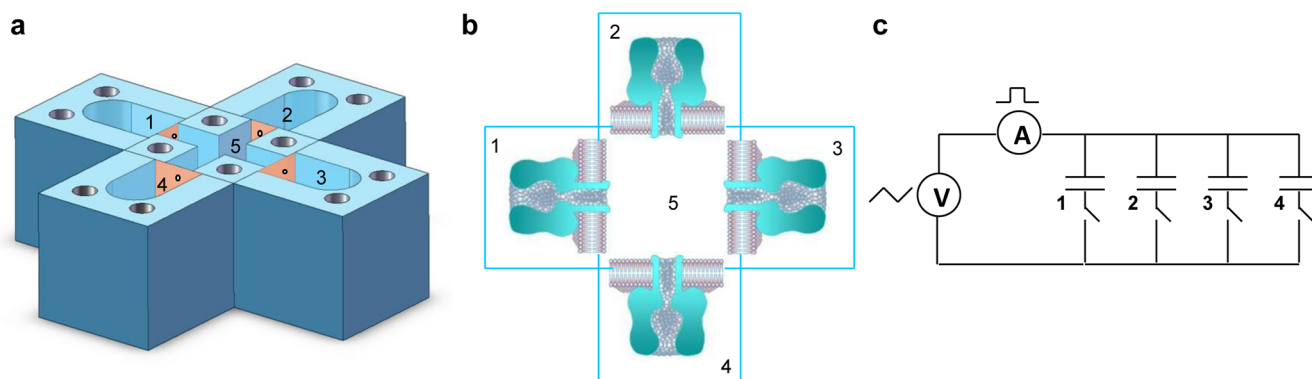


**FIGURE 9.** Illustration of a pattern-recognition stochastic sensor consisting of four protein nanopores: (a) chamber device, which consists of four *cis* compartments (labeled as 1, 2, 3, and 4), and one *trans* compartment (labeled as 5); (b) schematic configuration of the four proteins after their insertion into the lipid bilayers formed on the apertures of the Teflon films which separate the *cis* and *trans* compartments; and (c) circuit diagram of the pattern-recognition stochastic sensor, in which four switches were used to control component sensor(s) to be monitored. Reprinted with permission from ref 48. Copyright 2009 Institute of Physics.

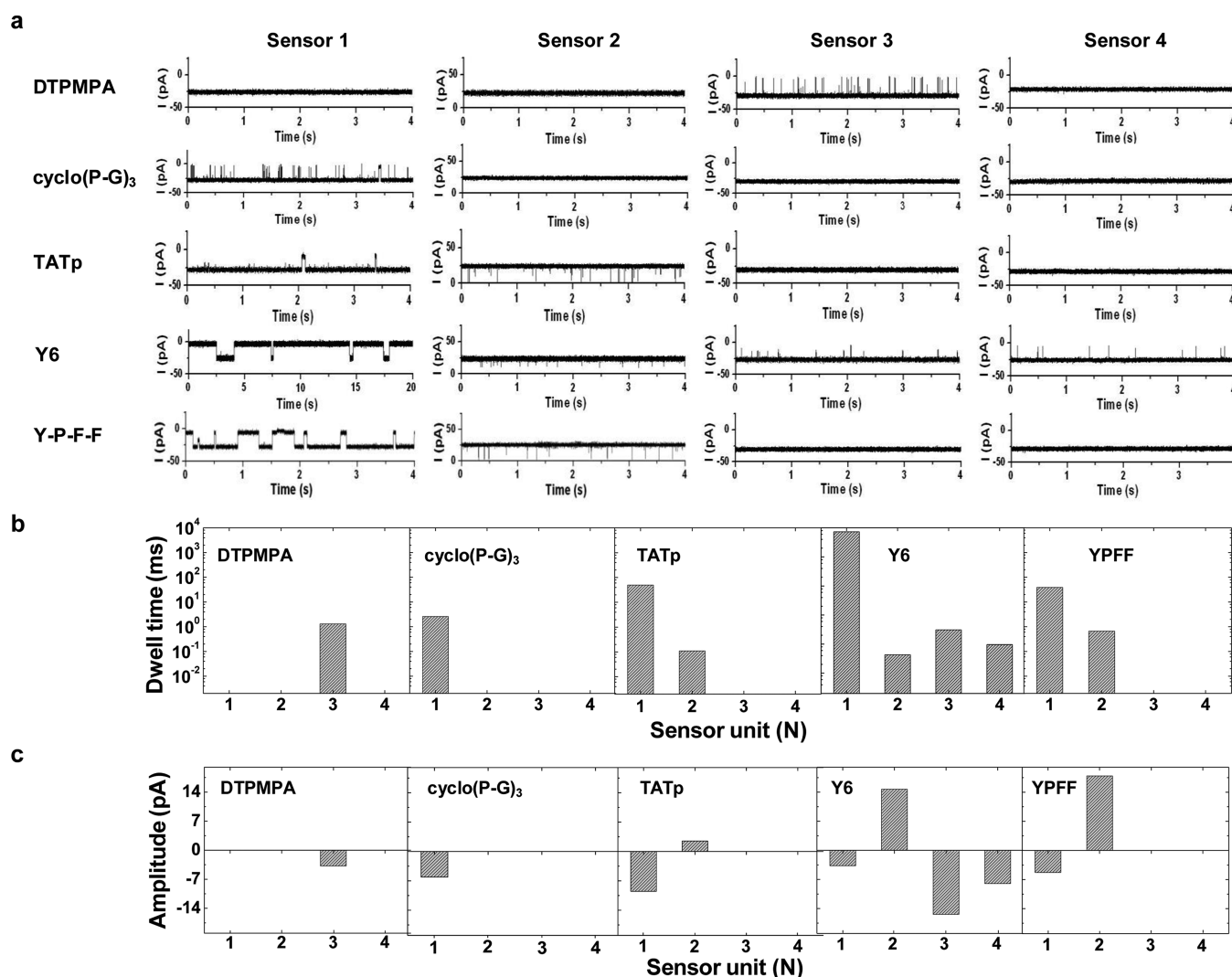


**FIGURE 10.** Pattern-recognition differentiation of a variety of molecules: (a) electrical recordings showing the current blockages of various analytes in the four component pores of the pattern-recognition stochastic sensor; the corresponding (b) dwell time plot and (c) amplitude plot. Reprinted with permission from ref 48. Copyright 2009 Institute of Physics.



examined.<sup>29,30,43–45</sup> We found that utilizing ionic liquid BMIM-Cl solution as the background electrolyte instead of NaCl/KCl resulted in ~2 orders of magnitude reduction in the velocity of DNA translocation through protein pores (Figure 8).<sup>43</sup> Compared with other physical conditions, such as temperature, ionic strength, viscosity, etc., the effect of organic salts on DNA translocation was far more significant.

**Development of Pattern-Recognition Nanopore Sensor Array.** The mammalian olfactory system can distinguish thousands of individual odors by using an array of nonspecific cross-reactive receptors with different affinities for analytes of interest.<sup>46</sup> In such a system, an odor is sensed by millions of sensory receptor neurons in the olfactory epithelium, and the resulting temporal response pattern from many receptor cells is then transmitted to the brain, where pattern recognition methods are used to identify, classify, and quantify the odor of interest. This biological sensing principle has been employed by bioinspired, artificial olfactory systems (well-known as “electronic nose”), which consist of an array of semiselective sensors to identify and discriminate different organic compounds (“odors”) based on a pattern-recognition algorithm.<sup>47</sup> Such a biological sensing principle was recently employed by our group to improve the resolution of nanopore analysis.<sup>48</sup> In the constructed pattern-recognition nanopore sensor, an array of protein pores modified with a variety of noncovalent bonding sites were used as the sensing elements (Figure 9). Five compounds were examined, including organophosphate diethylenetriaminepentamethylenephosphonic acid (DTPMPA), as well as four peptides: cyclo(P-G)<sub>3</sub>, YYYYYY (Y6), YPFF, and HIV-1 TAT protein peptide (TATp) with a sequence of YGRKKRRQRRR. The collective responses of each individual component nanopore to a compound (Figure 10a) produce diagnostic patterns characterized by event residence time (Figure 10b) and amplitude (Figure 10c), which can independently or collectively serve as an analyte signature(s). With an increase in the dimensionality of the signal, the nanopore sensor array provided an enhanced resolution for the differentiation of analytes compared with a single-pore configuration.<sup>48</sup>

## Concluding Remarks

Nanopore stochastic sensing has shown great potential as an emerging science and technology for various applications. However, two major issues need to be addressed in order to transition the currently available nanopore technology to deployable sensors for the analysis of real-world samples. First, most of the nanopore stochastic sensors reported thus far rely on weak noncovalent bonding

interactions to detect analytes and hence are only semiselective. It is likely that a number of matrix components in the real-world samples will potentially interfere with the detection of target analytes. In addition to constructing a pattern-recognition nanopore sensor array to improve the sensor resolution, another viable approach to overcome the matrix effect is to develop functionalized nanopores possessing highly selective binding sites. For example, such pores can be produced by attaching aptamers, antibodies, or other ligands to the pore interior. Alternatively, selective nanopore sensors can be constructed by self-assembly of supramolecules. Such synthetic nanopore or lipid bilayer based sensing systems have successfully been constructed to detect enzyme activity and differentiate odorants.<sup>49,50</sup> Further, nanopore sensors can be coupled with chromatography, thus offering great promise to the selective detection of the target analyte. Second, various applications of the nanopores reported so far have mainly been achieved using protein ion channels. The high sensitivity and selectivity of these biological nanopores are accomplished based on modification of the nanopore interior to introduce a variety of new functions at specific positions. However, the protein pore-based stochastic sensing is not suitable as deployable tools for extended usage due to the fragility of the biological membranes used in such sensing platforms. Development of artificial nanopores in robust solid-state substrates offers great potential as portable/fieldable stochastic sensors. These artificial pores have many advantages over the biological pores. For example, they can have flexible pore diameters and lengths, function in a variety of extreme conditions, and be used repetitively. However, the currently available artificial pore technology provides a poor resolution and selectivity due to the difficulty in imparting these nanopores with surface functionalities. Although significant advancements have been made in the introduction of selectivity and chemical functions to solid-state nanopores,<sup>51–53</sup> new techniques are still needed for this effort.

---

*This research was financially supported by the Defense Advanced Research Projects Agency, the Department of Homeland Security, the National Institutes of Health, and the National Science Foundation. We are thankful for members of our laboratories, past and present, who contributed significantly to the research discussed here.*

---

## BIOGRAPHICAL INFORMATION

**Guihua Wang** is an Associate Professor in the School of Chemistry and Biological Engineering at University of Science and Technology Beijing (USTB). She received her Ph.D. degree in Physical Chemistry in 2007 from USTB and did her postdoctoral

research at the University of Texas at Arlington from January 2011 to October 2012. Currently, Dr. Wang is a senior research associate in the Department of Biological and Chemical Sciences at the Illinois Institute of Technology. Her research activities include the study of kinetics of electrode reactions both in aqueous and in nonaqueous media and the development of nanopore stochastic sensing techniques for the detection of biomolecules.

**Liang Wang** is a senior research associate in the Department of Biological and Chemical Sciences at Illinois Institute of Technology, where he works with Prof. Guan on nanopore stochastic sensing. He obtained his Ph.D. in Biochemistry and Molecular Biology in 2011 from Institute for Nanobiomedical Technology and Membrane Biology, Sichuan University, P.R. China, where he studied molecular self-assembling systems using peptides motifs, and then worked at Jiangsu University as a research associate.

**Yujing Han** received her B.S. degree in Biochemistry and Biotechnology in 2011 from Florida Institute of Technology and Shanghai Ocean University, P. R. China. She is currently a graduate student in the Department of Biological and Chemical Sciences at Illinois Institute of Technology.

**Shuo Zhou** is a graduate student in the Department of Biological and Chemical Sciences at Illinois Institute of Technology. She received her B.S. degree in Chemistry from Yunnan University, P.R. China, in 2010.

**Xiyun Guan** is an Associate Professor in the Department of Biological and Chemical Sciences at the Illinois Institute of Technology. He obtained his Ph.D. in Chemistry at the University of Kentucky, Lexington, in 2002. Then, he worked as a postdoctoral research associate in the Department of Medical Biochemistry and Genetics at Texas A&M Health Science Center, and an Assistant Professor in the Department of Chemistry and Biochemistry at the University of Texas at Arlington. His current research focuses on the development of nanopore techniques for applications in biotechnology at the single molecule level.

#### FOOTNOTES

The authors declare no competing financial interest.

#### REFERENCES

- Bayley, H.; Cremer, P. S. Stochastic Sensors Inspired by Biology. *Nature* **2001**, *413*, 226–230.
- Coulter, W. H. Means for Counting Particles Suspended in a Fluid. U.S. Patent 2,656,508 1953.
- Dutzler, R. The Structural Basis of ClC Chloride Channel Function. *Trends Neurosci.* **2004**, *27*, 315–320.
- Wang, G.; Zhang, B.; Wayment, J. R.; Harris, J. M.; White, H. S. Electrostatic-Gated Transport in Chemically Modified Glass Nanopore Electrodes. *J. Am. Chem. Soc.* **2006**, *128*, 7679–7686.
- Zhao, Q.; Jayawardhana, D. A.; Wang, D.; Guan, X. Study of Peptide Transport through Engineered Protein Channels. *J. Phys. Chem. B* **2009**, *113*, 3572–3578.
- Kang, X.; Gu, L.; Cheley, S.; Bayley, H. Single Protein Pores Containing Molecular Adapter at High Temperature. *Angew. Chem., Int. Ed.* **2005**, *44*, 1495–1499.
- de Zoysa, R. S. S.; Krishantha, D. M. M.; Zhao, Q.; Gupta, J.; Guan, X. Translocation of Single Stranded DNA through the Alpha-Hemolysin Nanopore in Acidic Solutions. *Electrophoresis* **2011**, *32*, 3034–3041.
- Meller, A.; Nivon, L.; Branton, D. Voltage-Driven DNA Translocations through a Nanopore. *Phys. Rev. Lett.* **2001**, *86*, 3435–3438.
- Kuyucak, S.; Bastug, T. Physics of Ion Channels. *J. Biol. Phys.* **2003**, *29*, 429–446.
- Cheley, S.; Gu, L.; Bayley, H. Stochastic Sensing of Nanomolar Inositol 1,4,5-Trisphosphate with an Engineered Pore. *Chem. Biol.* **2002**, *9*, 829–838.
- Liu, A.; Zhao, Q.; Krishantha, D. M. M.; Guan, X. Unzipping of Double-stranded DNA in Engineered Protein Pores. *J. Phys. Chem. Lett.* **2011**, *2*, 1372–1376.
- Gu, L.; Braha, O.; Conlan, S.; Cheley, S.; Bayley, H. Stochastic Sensing of Organic Analytes by a Pore-Forming Protein Containing a Molecular Adapter. *Nature* **1999**, *398*, 686–690.
- Jayawardhana, D. A.; Crank, J. A.; Zhao, Q.; Armstrong, D. W.; Guan, X. Nanopore Stochastic Detection of a Liquid Explosive Component and Sensitizers Using Boromycin and an Ionic Liquid Supporting Electrolyte. *Anal. Chem.* **2009**, *81*, 460–464.
- Braha, O.; Webb, J.; Gu, L.; Kim, K.; Bayley, H. Carriers versus Adapters in Stochastic Sensing. *ChemPhysChem* **2005**, *6*, 889–892.
- Guan, X.; Gu, L.; Cheley, S.; Braha, O.; Bayley, H. Stochastic Sensing of TNT with a Genetically Engineered Pore. *ChemBioChem* **2005**, *6*, 1875–1881.
- Braha, O.; Walker, B.; Cheley, S.; Kasianowicz, J. J.; Song, L.; Gouaux, J. E.; Bayley, H. Designed Protein Pores as Components for Biosensors. *Chem. Biol.* **1997**, *4*, 497–505.
- Gao, C.; Ding, S.; Tan, Q.; Gu, L. Method of Creating a Nanopore-Terminated Probe for Single-Molecule Enantiomer Discrimination. *Anal. Chem.* **2009**, *81*, 80–86.
- Lee, S. B.; Mitchell, D. T.; Trofin, L.; Nevanen, T. K.; Soderlund, H.; Martin, C. R. Antibody-Based Bio-Nanotube Membranes for Enantiomeric Drug Separations. *Science* **2002**, *296*, 2198–2200.
- Ding, S.; Gao, C.; Gu, L. Capturing Single Molecules of Immunoglobulin and Ricin with an Aptamer-Encoded Glass Nanopore. *Anal. Chem.* **2009**, *81*, 6649–6655.
- Siwy, Z.; Trofin, L.; Kohli, P.; Baker, L. A.; Trautmann, C.; Martin, C. R. Protein Biosensors Based on Biofunctionalized Conical Gold Nanotubes. *J. Am. Chem. Soc.* **2005**, *127*, 5000–5001.
- Sexton, L. T.; Horne, L. P.; Sherrill, S. A.; Bishop, G. W.; Baker, L. A.; Martin, C. R. Resistive-Pulse Studies of Proteins and Protein/Antibody Complexes Using a Conical Nanotube Sensor. *J. Am. Chem. Soc.* **2007**, *129*, 13144–13152.
- Luchian, T.; Shin, S. H.; Bayley, H. Single-Molecule Covalent Chemistry with Spatially Separated Reactants. *Angew. Chem., Int. Ed.* **2003**, *42*, 3766–3771.
- Zhao, Q.; Jayawardhana, D. A.; Guan, X. Stochastic Study of the Effect of Ionic Strength on Noncovalent Interactions in Protein Pores. *Biophys. J.* **2008**, *94*, 1267–1275.
- Shim, J. W.; Tan, Q.; Gu, L. Single-Molecule Detection of Folding and Unfolding of the G-Quadruplex Aptamer in a Nanopore Nanocavity. *Nucleic Acids Res.* **2009**, *37*, 972–982.
- Talaga, D. S.; Li, J. Single-Molecule Protein Unfolding in Solid State Nanopores. *J. Am. Chem. Soc.* **2009**, *131*, 9287–9297.
- Kasianowicz, J. J.; Brandin, E.; Branton, D.; Deamer, D. Characterization of Individual Polynucleotide Molecules Using a Membrane Channel. *Proc. Natl. Acad. Sci. U. S. A.* **1996**, *93*, 13770–13773.
- Meller, A.; Nivon, L.; Brandin, E.; Golovchenko, J.; Branton, D. Rapid Nanopore Discrimination between Single Polynucleotide Molecules. *Proc. Natl. Acad. Sci. U. S. A.* **2000**, *97*, 1079–1084.
- Howorka, S.; Cheley, S.; Bayley, H. Sequence-Specific Detection of Individual DNA Strands Using Engineered Nanopores. *Nat. Biotechnol.* **2001**, *19*, 636–639.
- Storm, A. J.; Storm, C.; Chen, J.; Zandbergen, H.; Joanny, J. F.; Dekker, C. Fast DNA Translocation through a Solid-State Nanopore. *Nano Lett.* **2005**, *5*, 1193–1197.
- Sigalov, G.; Comer, J.; Timp, G.; Aksimentiev, A. Detection of DNA Sequences Using an Alternating Electric Field in a Nanopore Capacitor. *Nano Lett.* **2008**, *8*, 56–63.
- Jovanovic-Talisman, T.; Tetenbaum-Novatt, J.; McKenney, A. S.; Zilman, A.; Peters, R.; Rout, M. P.; Chait, B. T. Artificial Nanopores that Mimic the Transport Selectivity of the Nuclear Pore Complex. *Nature* **2009**, *457*, 1023–1027.
- Derrington, I. M.; Butler, T. Z.; Collins, M. D.; Manrao, E.; Pavlenok, M.; Niederweis, M.; Gundlach, J. H. Nanopore DNA Sequencing with MspA. *Proc. Natl. Acad. Sci. U. S. A.* **2010**, *107*, 16060–16065.
- Schmidt, J. Stochastic Sensors. *J. Mater. Chem.* **2005**, *15*, 831–840.
- Howorka, S.; Siwy, Z. Nanopore Analytics: Sensing of Single Molecules. *Chem. Soc. Rev.* **2009**, *38*, 2360–2384.
- Venkatesan, B. M.; Bashir, R. Nanopore Sensors for Nucleic Acid Analysis. *Nat. Nanotechnol.* **2012**, *7*, 615–624.
- Wanunu, M. Nanopores: A Journey towards DNA Sequencing. *Phys. Life Rev.* **2012**, *9*, 125–158.
- Kang, X.; Cheley, S.; Guan, X.; Bayley, H. Stochastic Detection of Enantiomers. *J. Am. Chem. Soc.* **2006**, *128*, 10684–10685.
- Zhao, Q.; Wang, D.; Jayawardhana, D. A.; de Zoysa, R. S. S.; Guan, X. Real-Time Monitoring of Peptide Cleavage Using a Nanopore Probe. *J. Am. Chem. Soc.* **2009**, *131*, 6324–6325.
- Krishantha, D. M. M.; Breitbach, Z. S.; Padivitage, N. L. T.; Armstrong, D. W.; Guan, X. Rapid Determination of Sample Purity and Composition by Nanopore Stochastic Sensing. *Nanoscale* **2011**, *3*, 4593–4596.
- Wang, D.; Zhao, Q.; de Zoysa, R. S. S.; Guan, X. Detection of Nerve Agent Hydrolytes in an Engineered Nanopore. *Sens. Actuators, B* **2009**, *139*, 440–446.
- Gupta, J.; Zhao, Q.; Wang, G.; Kang, X.; Guan, X. Simultaneous Detection of CMPA and PMPA, Hydrolytes of Soman and Cyclosarin Nerve Agents, by Nanopore Analysis. *Sens. Actuators, B* **2013**, *176*, 625–631.

- 42 Modi, N.; Singh, P. R.; Mahendran, K. R.; Schulz, R.; Winterhalter, M.; Kleinekath, U. Probing the Transport of Ionic Liquids in Aqueous Solution through Nanopores. *J. Phys. Chem. Lett.* **2011**, *2*, 2331–2336.
- 43 de Zoysa, R. S. S.; Jayawardhana, D. A.; Zhao, Q.; Wang, D.; Armstrong, D. W.; Guan, X. Slowing DNA Translocation through Nanopores Using a Solution Containing Organic Salts. *J. Phys. Chem. B* **2009**, *113*, 13332–13336.
- 44 Bhattacharya, S.; Derrington, I. M.; Pavlenok, M.; Niederweis, M.; Gundlach, J. H.; Aksimentiev, A. Molecular Dynamics Study of MspA Arginine Mutants Predicts Slow DNA Translocations and Ion Current Blockades Indicative of DNA Sequence. *ACS Nano* **2012**, *6*, 6960–6968.
- 45 Luan, B.; Stolovitzky, G.; Martyna, G. Slowing and Controlling the Translocation of DNA in a Solid-State Nanopore. *Nanoscale* **2012**, *4*, 1068–1077.
- 46 Dickinson, T. A.; White, J.; Kauer, J. S.; Walt, D. R. Current Trends in 'Artificial-Nose' Technology. *Trends Biotechnol.* **1998**, *16*, 250–258.
- 47 Turner, A. P.; Magan, N. Electronic Noses and Disease Diagnostics. *Nat. Rev. Microbiol.* **2004**, *2*, 161–166.
- 48 Zhao, Q.; Wang, D.; Jayawardhana, D. A.; Guan, X. Stochastic Sensing of Biomolecules in a Nanopore Sensor Array. *Nanotechnology* **2008**, *19*, No. 505504.
- 49 Das, G.; Talukdar, P.; Matile, S. Fluorometric Detection of Enzyme Activity with Synthetic Supramolecular Pores. *Science* **2002**, *298*, 1600–1602.
- 50 Takeuchi, T.; Montenegro, J.; Hennig, A.; Matile, S. Pattern Generation with Synthetic Sensing Systems in Lipid Bilayer Membranes. *Chem. Sci.* **2011**, *2*, 303–307.
- 51 Wei, R.; Gatterdam, V.; Wieneke, R.; Tampé, R.; Rant, U. Stochastic Sensing of Proteins with Receptor-Modified Solid-State Nanopores. *Nat Nanotechnol.* **2012**, *7*, 257–263.
- 52 Nasir, S.; Ali, M.; Ensinger, W. Thermally Controlled Permeation of Ionic Molecules through Synthetic Nanopores Functionalized with Amine-Terminated Polymer Brushes. *Nanotechnology* **2012**, *23*, No. 225502.
- 53 Pardon, G.; Gatty, H. K.; Stemme, G.; van der Wijngaart, W.; Roxhed, N. Pt-Al<sub>2</sub>O<sub>3</sub> Dual Layer Atomic Layer Deposition Coating in High Aspect Ratio Nanopores. *Nanotechnology* **2013**, *24*, No. 015602.